Acta Cryst. (1962). **15**, 1125

Experimental Determination of Extinction in Crystals

By J. J. De Marco and R. J. Weiss

Materials Research Laboratory, U.S. Army Materials Research Agency, Watertown 72, Massachusetts, U.S.A.

(*Received* 6 *October* 1961 *and in revised form* 19 *February* 1962)

X-ray measurements of the integrated intensities of Fe single crystals and Fe powders support the idealized mosaic block model for calculating extinction. Secondary extinction was shown to be predominant in these specimens. Expressions are given which can serve as a guide for estimating extinction and for selecting those parameters which minimize extinction.

Introduction

In this paper we report the results of measurements on single crystals and powders undertaken to compare the observed diffracted intensities with those calculated for the traditional mosaic block model of a crystal. The mosaic block model was introduced by Darwin (1914) solely for mathematical convenience. Today we have an approximate idea of the structure of an imperfect crystal in terms of arrays of dislocations but such a realistic case is mathematically untractable. It behooves us, then, to pursue the crude mosaic block model since it may yield mathematical expressions which intrinsically contain the physics of the problem and are accurate enough for the bulk of the problems encountered by the X-ray physicist and crystallographer.

In the mosaic block model a single crystal is divided into approximately equal small blocks (dimension $\sim t_0$) with neighboring blocks tilted with respect to each other so they do not simultaneously satisfy the Bragg conditions for any specific X-ray. Each mosaic block consists of a perfect array of atoms. The crystal is described, then, in terms of the size of the blocks and the angular distribution between the blocks. For convenience the regions of misfit between the blocks is considered void.

In calculating the integrated intensity of X-rays diffracted from a crystal one implicitly proceeds by calculating the diffraction from a free atom first. The amplitude of the scattered wave (in units of e^2/mc^2) is commonly called the atomic scattering factor, f, and the intensity of scattered X-rays is proportional to $f^2(e^2/mc^2)^2$. When the atom becomes part of a crystal the scattered amplitude of a unit cell of that crystal is called the structure factor, $F(e^2/mc^2)$, and is a sum of the atomic scattering factors of the atoms in the unit cell weighted according to their phases. The calculation of the integrated intensity of a Bragg reflection of a crystal, however, can be beset with difficulties. Only in the limit of extremely small mosaic blocks and very large angular tilts between the mosaic blocks is the integrated intensity proportional to $F^2(e^2/mc^2)^2$. For such a single crystal in symmetrical reflection the integrated intensity, E, of a Bragg reflection is *independent of the size and angular distribution of the mosaic blocks* and is given by

$$E\omega/I = |F|^2(e^2/mc^2)^2\lambda^3N^2(1+\cos^2 2\theta)/(2\sin 2\theta) \\ \times (\exp[-2M]/2\mu) = \bar{Q}/2\mu \quad (1)$$

ideally imperfect single crystal in symmetrical reflection.

Equation (1) is derived for a crystal intercepting the entire monochromatic X-ray beam (wavelength λ) and one thick enough so that the entire X-ray beam is attenuated. N is the number of unit cells per cubic centimeter, $\exp[-2M]$ the Debye–Waller temperature factor, θ the Bragg angle, ω the angular velocity of the crystal as it is rotated through the Bragg angle, I the number of monochromatic X-rays per unit time incident upon the crystal and μ the linear absorption coefficient commonly determined by measuring the exponential attenuation of a thin foil of the material. The factor $(1+\cos^2 2\theta)/2$ represents the average over the directions of polarization of an initially unpolarized beam incident upon the crystal.

If the crystal is perfect (one large mosaic block) the integrated intensity of an initially unpolarized beam is again calculable and is now proportional to $F(e^2/mc^2)$. It is

$$\frac{E\omega}{I} \cong \frac{8|F|e^2\lambda^2N\exp[-M]}{3\pi mc^2\sin 2\theta} \\ \times [(1-2\varkappa_\sigma)+\cos 2\theta(1-2\varkappa_\pi)] \quad (2)$$

ideally perfect crystal in symmetrical reflection

where the terms $\varkappa_\sigma(=\mu/2|F|N\lambda\exp[-M]e^2/mc^2)$ and $\varkappa_\pi(=\mu/2|F|N\lambda\cos 2\theta\exp[-M]e^2/mc^2)$ account for the absorption in the crystal of the two states of polarization and are generally small. As in the ideally imperfect crystal, equation (2) applies to the case of a symmetrically cut thick crystal intercepting the entire X-ray beam. Since the physicist and crystallographer are generally interested in determining F, either an ideally imperfect or an ideally perfect crystal will suffice for this measurement. For a particular Bragg reflection the ideally imperfect crystal (equation (1)) gives the maximum integrated intensity and the ideally perfect crystal (equation (2)) gives the minimum, the ratios generally being about an order of magnitude. All real crystals, though, give an integrated intensity somewhere between equations (1) and (2) and any reduction in integrated intensity from that given by equation (1) is called *extinction*. The determination of the integrated intensity in these intermediate cases in our present interest.

It is traditional to consider two types of extinction, one in which the mosaic blocks become too large, commonly called *primary extinction* and one in which the angular distribution between blocks becomes too small, commonly called *secondary extinction*. In principle either one or both can be present. Conceptually one can understand extinction by bearing in mind that equation (1) is derived for the case where Bragg scattering is so weak that the X-ray beam is attenuated almost entirely by processes other than Bragg scattering (like fluorescence and Compton scattering). If the mosaic blocks become too large or if the angular distribution of mosaic blocks becomes too small then Bragg scattering may comprise a significant fraction of the attenuation when the crystal is set at the Bragg angle. Under these conditions the scattered wave may undergo a second (or further) Bragg scattering before it emerges from the crystal and this reduces the integrated intensity entering the counter. In order to calculate the integrated intensity within the framework of the mosaic block model *one must know the size and angular distribution of mosaic blocks.* Unfortunately one can not always determine these quantities independently.

In proceeding with this problem it is convenient to consider our measurements on single crystals and powders separately since the single crystal case affords us the possibility of measuring separately the approximate angular distribution of mosaic blocks. This leaves the mosaic block size t_0 as the only unknown in evaluating the data whereas there are three unknowns in evaluating the powder data (see below).

Single crystals

It has generally been assumed and our measurements concur that the angular distribution of mosaic blocks can be approximated by the Gaussian distribution

$$W(\Delta) = \sqrt{(2)}g \exp(-2\pi g^2 \Delta^2) \qquad (3)$$

angular distribution of mosaic blocks

where Δ is the angular deviation from the peak in the distribution function, and $0{\cdot}664/g$. is the full width at half maximum. For such a Gaussian distribution of very small mosaic blocks the right side of equation (1) is reduced by the secondary extinction factor*

$$S \cong [1 + 0{\cdot}87(\bar{Q}g/\mu) - 0{\cdot}08(\bar{Q}g/\mu)^2]^{-1} \qquad (4)$$

secondary extinction factor for thick crystals.

If this factor is very close to unity ($\bar{Q}g/\mu \ll 1$) then the crystal is devoid of secondary extinction and equation (1) can be used directly†.

If the mosaic blocks are not very small then equation (1) is reduced by the primary extinction factor approximately given as

$$P \cong (\tanh A)/A$$
$$A = (e^2/mc^2)(\lambda|F|t_0NK \exp[-M]) \qquad (5)$$

primary extinction factor,
Zachariasen (1944) *equation* (3·167)

where t_0 is the size of the mosaic blocks. If neither primary nor secondary extinction are negligible then the right side of equation (1) is multiplied by the product of S and P.

In principle it is possible to measure independently the unknown parameters in S and P (i.e. g and t_0). g can be measured from the shape of the rocking curve while t_0 can be measured from the true width, $\Delta\theta$, of the diffracted line by using the well known expression

$$\Delta\theta \cong \lambda/t_0 \cos\theta\ . \qquad (6)$$

In practice, though, only the shape of the rocking curve is readily measured. If t_0 is large enough to give appreciable primary extinction ($t_0 > 10^{-4}$ cm.) then $\Delta\theta$ is too small to measure without considerable effort.

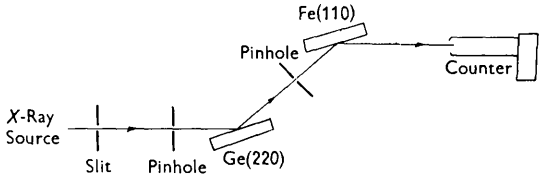

Fig. 1. A schematic diagram of the geometrical arrangement in the single-crystal measurements.

It is assumed in the derivation of equation (4) that each X-ray experiences the distribution function of equation (3) as it penetrates the crystal. Since the depth of penetration is approximately $1/\mu$ it is desirable to measure the rocking curve with a beam of X-rays illuminating an area of the crystal no larger than $\sim (1/\mu)^2$. If the X-ray beam illuminates too large an area then large scale distortions or non-uniform distributions of g will yield an apparent rocking curve that is too large. Thus in our experiment the beam was made to pass through two pin holes

---

* This factor represents a graphical integration of equation (4·27) of Zachariasen (1944).

† Equations (1) and (4) are correct for any specific photon, providing $(1+\cos^2 2\theta)/2$ is replaced by the appropriate polarization factor K^2, ($\cos^2 2\theta$ and unity) for the two states of polarization. One then must average over the directions of polarization. The factor $(1+\cos^2 2\theta)/2$ in equation (1) is correct if $S = 1$ (no secondary extinction) but a proper averaging of the polarization for $S \neq 1$ leads to more cumbersome expressions. Since equation (4) is a slowly varying function of $\bar{Q}$ the use of equations (1) and (4) as they are given will lead to errors of no more than about 15% in S. For accurate work, though, this matter must be considered.

(Fig. 1) so that the illuminated area was approximately 10^{-4} cm.^{2}. An ideally perfect Ge (220) crystal was chosen for the monochromator since it has a very narrow rocking curve and its lattice spacing is close to the lattice spacing of our sample, Fe(110), [Ge(220) $d=2{\cdot}00$ Å; Fe(110) $d=2{\cdot}04$ Å]. The similarity in lattice spacings and the use of the crystals in the parallel position (Fig. 1) virtually eliminated all errors due to the finite geometrical and wavelength resolution. The data is placed on an absolute basis by measuring directly the intensity of the monochromatic radiation diffracted from the Ge crystal. Uncertainties in the atomic scattering factor and Hönl (dispersion) corrections for Fe lead to errors of about 3% in calculating E from equation (1) but this is small compared to the scatter in our data.

There are three parameters in equations (4) and (5) that can be varied in a measurable fashion; λ, the wavelength; 0·664/g., the width of the angular distribution of mosaic blocks; and F, the structure factor. However, the dependence of S and P on F are quite similar and such variation offers little opportunity to assess the relative contribution of primary and secondary extinction. On the other hand the wavelength dependence is markedly different since P approaches unity as λ approaches zero and S approaches zero as λ approaches zero. While the wavelength dependence alone can distinguish qualitatively between the cases of primary and secondary extinction, only a measure of g and t_0 can provide all the quantities required for an absolute determination of the integrated intensity. Only g was determined in the present experiment and it was varied by selecting different spots on the surface of the crystal. An evaluation of the data, though, was not unduly hampered by the lack of an independent measurement of t_0 since t_0 was apparently not too large in our samples.

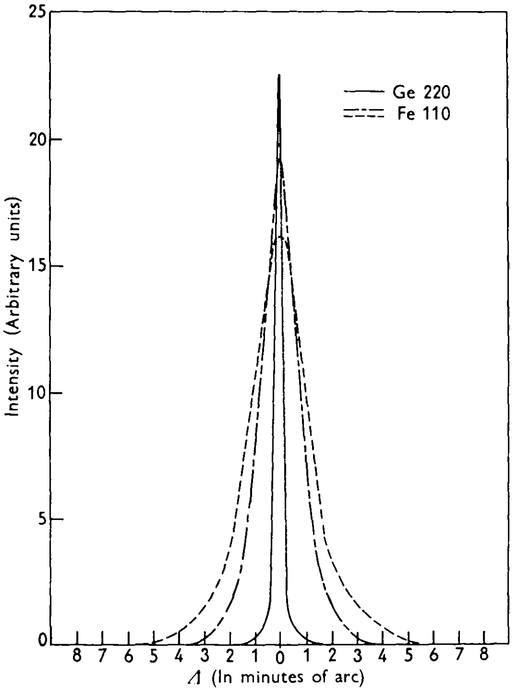

Fig. 2. The rocking curve (1, −1) of a Ge (220) crystal and of two spots on the Fe (110) crystal used in our measurements. Cu $K\alpha$ radiation was employed with the geometry of Fig. 1.

Two Fe crystals were employed, both grown from the melt by the addition of a small percentage ($\sim$ 1·5 at.%) of Al to close the γ loop. One crystal had a rocking curve of approximately two min. of arc, quite narrow for a crystal grown from the melt, and the second crystal was cold rolled to increase the rocking curve to about fifteen min. of arc. In Fig. 2 are shown two of the rocking curves of the first iron crystal taken with Cu $K\alpha$ radiation at two different spots on the surface. Variations in width by as much as a factor of two were observed over the surface. The rocking curve of an ideally perfect Ge (220) crystal is shown for comparison. Its full width at half maximum (20 sec.) compares favorably with the calculated compound width of 19 sec. for the double crystal arrangement ($\sim$ 13 sec. for a single ideally perfect Ge (220) crystal).

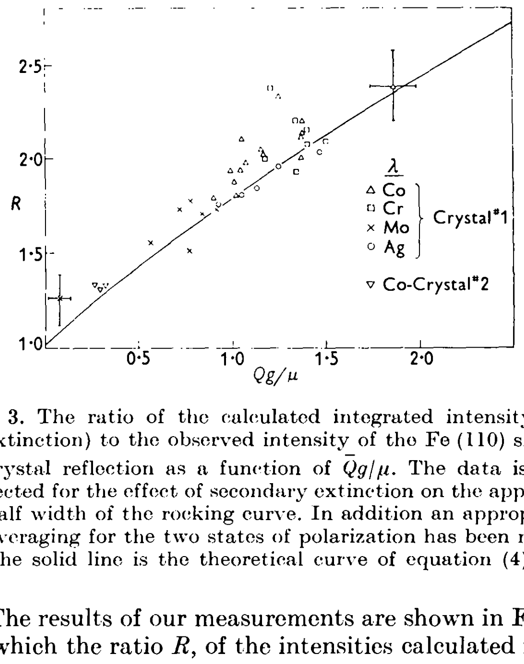

Fig. 3. The ratio of the calculated integrated intensity (no extinction) to the observed intensity of the Fe (110) single-crystal reflection as a function of $\bar{Q}g/\mu$. The data is corrected for the effect of secondary extinction on the apparent half width of the rocking curve. In addition an appropriate averaging for the two states of polarization has been made. The solid line is the theoretical curve of equation (4).

The results of our measurements are shown in Fig. 3 in which the ratio R, of the intensities calculated from equation (1) to the observed intensities are plotted as a function of ($\bar{Q}g/\mu$) the argument in equation (4). The reciprocal of this ratio directly yields the product of P and S, i.e.

$$R = \frac{\text{calculated intensity (equation (1))}}{\text{observed intensity}} = \frac{1}{P \times S} \tag{7}$$

Since g for each point in Fig. 3 is obtained from the observed widths at half maximum a correction must be applied since secondary extinction distorts the line shape. In the presence of secondary extinction the peak of the rocking curve is reduced more than the wings so that there is an apparent increase in the width. In symmetrical reflection the true width at half maximum of a thick crystal is related to the observed width by

$$\text{Observed width/True width} \simeq 1 + 0{\cdot}31\,(\bar{Q}g/\mu) - 0{\cdot}065\,(\bar{Q}g/\mu)^2 \tag{8}$$

graphical integration of equation (4·27), *Zachariasen* (1944).

The maximum correction applied to the data of Fig. 3 is about 30% in width.

Over a wide range of values of R a superficial inspection of the data in Fig. 3 indicates a general agreement between theory and experiment by setting $P=1$ (no primary extinction, secondary extinction only). That the data could not be fitted to an expression for primary extinction only ($S=1$) can be seen from inspection. If only primary extinction were present the values of R would increase monotonically with increasing wavelength whereas we see an inversion between Mo $K\alpha$ (0·71 Å) and Ag $K\alpha$ (0·56 Å). In addition the data for Co $K\alpha$ cover a range of values of $R=1{\cdot}7$ to $2{\cdot}3$ or values of t_0 in equation (5) of about $3{\cdot}2$ to $4{\cdot}6 \times 10^{-4}$ cm. while the data for the same crystal taken with Ag $K\alpha$ ($R=1{\cdot}8$ to $2{\cdot}0$) would require values of t_0 of $7{\cdot}5$ to $\sim 8{\cdot}7 \times 10^{-4}$ cm. Since the value of t_0 must be independent of the radiation chosen we must exclude the possibility of appreciable primary extinction.

Our conclusion is that secondary extinction is predominant in our crystals and the mosaic block model may be moderately successful for calculating integrated intensities in single crystals subject to extinction.

Powders

An evaluation of extinction in powders is considerably more complicated. In each powder particle any fraction of its volume that can be considered to be a single crystal no longer fulfills the conditions of a symmetrically cut thick crystal. In terms of the mosaic block model one would specify a powder sample according to the dimension of the mosaic blocks t_0, the angular distribution of the blocks (equation (3)), and the thickness, T, of the small volume in each powder particle that can be considered to be a single crystal. We shall assume these three parameters are approximately constant throughout each specimen to be examined. While the conditions of symmetrical reflection are not met one can average this in a powder sample. Unfortunately none of these three parameters are readily measurable in a powder specimen although one can set an upper limit to T as not to exceed the size of the individual particles in an unsintered powder specimen. Since the size of the mosaic blocks are a reflection of the internal state of perfection of the substance, it is also quite reasonable to assume that the size of the mosaic blocks are no larger in a powder specimen than in a single crystal (of the same material) that has been annealed in a similar manner. As primary extinction played a negligible role in our single crystal measurements we shall assume at the outset that this is the case for our powders so that we are primarily concerned with the two unknown parameters g and T. Again referring to equation (4·27) of Zachariasen we must calculate the integrated intensity of a crystal of finite thickness, T, averaged over the angle between the diffracting planes and the surface of the crystal (unsymmetrical reflection).[*] While we have been unable to evaluate this in closed form an approximate analytic fit (good to about 20%) leads to a ratio of integrated intensity without extinction to the integrated intensity with extinction given by

$$R \simeq [(1+\tfrac{1}{2}\mu T + g\bar{Q}T)/(1+\tfrac{1}{2}\mu T)] \tag{9}$$

secondary extinction in powders.

The experimental study of extinction in powders was made on Fe powders by comparing the integrated intensity ratios, R, of the first Bragg reflection from cold-worked samples to that from annealed samples as a function of X-ray wavelength (the cold-worked sample being essentially free of extinction). The experiments were made on 5 micron carbonyl Fe powder and 30 micron ferrovac Fe filings, two samples of each being lightly compressed to form a compact. One of each sample was left in a cold-worked state, the other was annealed at 850 °C. in vacuum for 1 hr. The intensities for the first Bragg reflection in each case were obtained with the following radiations: Ag $K\alpha$, Mo $K\alpha$, Cu $K\beta$ and $K\alpha$, Ni $K\alpha$, Co $K\alpha$ and Cr $K\alpha$. Except for the case of Mo $K\alpha$ which was monochromated by a single bent LiF crystal, all radiations were unfiltered. A sodium iodide, thallium-activated scintillation counter was used for detection, and a specimen spinner was used to rotate the sample in its own plane during the measurements.

The integrated intensities were taken to be directly proportional to the peak areas obtained by integrating a chart recording of the reflection over a sufficiently wide angular range such that the background appeared constant. While this method of integrating intensity measurements is dependent upon the selection of a background level, the errors tend to cancel since one is taking ratios of the same reflection. The thermal diffuse scattering correction for this reflection is negligible since the Debye–Waller factor is close to unity. In Table 1 the observed ratios are compared to those calculated from equation (9) with the param-

---

[*] For unsymmetrical reflection replace

$$\mu_0/\gamma_0 \text{ by } (\mu_0/2)(1-\gamma_0/|\gamma_H|)$$

in equation (4·27) of Zachariasen (1944).

Table 1. *The observed ratio,* R(obs.), *of the* 110 *integrated intensity of the cold-worked to annealed powder samples of ferrovac and carbonyl* Fe

These are compared to the ratios calculated from equation (9) with the parameter g and T adjusted to give a good fit. A value of $g = 1200$ corresponds to a mosaic block distribution of about 2 minutes in full width

			30 micron* ferrovac			5 micron* carbonyl Fe		
λ (Å)	$\bar{Q}$ (cm.$^{-1}$)	μ (cm.$^{-1}$)	R(obs.)	R(calc.)	Deviation	R(obs.)	R(calc.)	Deviation
2·291	1·03	906	2·22	2·22	—	3·64	3·34	−9%
1·791	0·538	465	1·83	1·80	−2%	3·19	3·11	−2%
1·659	0·710	3000	1·43	1·43	—	1·54	1·54	—
1·542	0·614	2500	1·49	1·42	−5%	1·61	1·55	−4%
1·392	0·495	1860	1·65	1·41	−17%	1·93	1·59	−21%
0·710	0·171	295	1·34	1·28	−5%	1·92	1·92	—
0·561	0·108	143	1·25	1·19	−5%	1·67	1·90	+14%
			$g = 1300$			$g = 1200$		
			$T = 1{\cdot}56 \times 10^{-3}$ cm.			$T = 1{\cdot}4 \times 10^{-2}$ cm.		

* The particle sizes given are for unannealed samples. After annealing considerable grain growth was observed in the carbonyl Fe due to sintering.

eters T and g adjusted to give a good fit for each sample. Over very wide ranges of R, Q, and μ equation (9) gives agreement to about 20%. Similar measurements were made on Cu and brass powders (Fig. 5) for which an even better fit was obtained but these powders did not provide as critical a test of equation (9) since wavelengths were not available for measurements close to either side of the absorption edge. Around the absorption edge $\bar{Q}$ varies smoothly and μ varies abruptly providing a good test of equation (9).

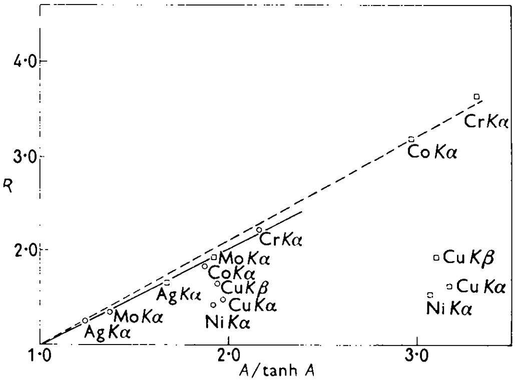

Fig. 4. The ratio of the integrated intensities of the 110 reflection in two samples of cold-worked and annealed Fe powders taken at various wave-lengths and plotted against the primary extinction correction $A/\tanh A$. (Circles: ferrovac; squares: carbonyl Fe).

An attempt was made to fit the iron powder data to the primary extinction expression of the form of equation (5) and this is shown in Fig. 4. The agreement is exceedingly poor in regions of high absorption. (An attempt to include absorption in equation (5) improved the agreement only slightly). No attempt was made to mix some primary extinction with the secondary extinction in order to improve the agreement in Table 1 since the theory is too crude to justify this.

Discussion

These results suggest that secondary extinction was predominant in our samples and that equations (4) and (9) provide a reasonable description of secondary extinction in single crystals and powders. Since the Fe single crystals selected for our measurements had a relatively high degree of perfection we believe these results have more general applicability. However one must be cautious not to apply equations (4) and (9) to samples whose degree of perfection approaches that of an ideally perfect crystal. Until more experimental data is available we suggest the use of equation (4) for single crystals whose rocking curve is at least twice as broad as that of a perfect crystal (full width at half maximum of an ideally perfect crystal $= 2N\lambda^2|F|(e^2/mc^2) \exp[-M]/\pi \sin 2\theta$).

As mentioned above, the crystallographer and physicist are interested in determining F, the structure factor, and to date no method providing an accurate correction for extinction is known.* In general the experimentalist wisely attempts to obtain samples free of extinction and we suggest that equations (4), (8) and (9) can serve as a guide. In the case of a single crystal a measurement of the rocking curve over an area $\sim (1/\mu)^2$ and a crude estimate of F enables one to evaluate extinction from equations (4) and (8) to within about 20%. If the sample and wavelength can be chosen so that S is estimated to be within 5% of unity then application of the secondary extinction correction (equation (4)) leads to an uncertainty of about 1%. If the extinction is considerably larger and accurate intensities are desired then an attempt must be made to alter the state of the crystal by plastic or elastic deformation. Once the absolute magnitude of F for the strong peaks is measured in a deformed crystal the weak outer peaks can be determined from an annealed crystal by determining the parameters

---

* If the extinction is small the method of Chandrasekhar (1960) in varying the polarization factor in equations (4) and (5) offers the possibility of making the correction.

of equation (4) from the extinction of the inner peaks. In addition a wavelength study may aid in evaluating the amount of extinction.

In the case of powders, equation (9) can serve as a guide for selecting the optimum conditions to minimize extinction but only a wavelength dependent study is really satisfactory in estimating the magnitude of R. Very fine cold-worked metal powders ($Z < 30$) appear to be free of extinction but a lack of extinction measurements on non-metallic powders forbids us from assessing the problem in such cases.

We shall conclude by mentioning some other work in this field. Weiss & DeMarco (1958) made a limited wavelength study of the integrated intensities of several crystals (from 0·5 Å to 0·9 Å) and employed a primary extinction correction (equation (5)). The absolute value of F was determined by extrapolating to zero wavelength, for which $P = 1$. From our current measurements it appears that this extrapolation was unjustified. *If secondary extinction is predominant in single crystals no procedure for extrapolation can correct for it.*

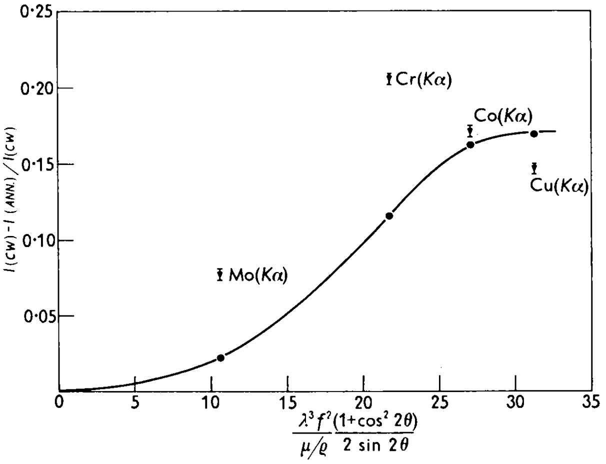

Fig. 5. The difference in integrated intensity of cold-worked and annealed α brass powders (divided by the cold-worked intensity) taken at various wave-lengths and plotted as a function of $\lambda^3 f^2 \varrho (1+\cos^2 2\theta)/2\mu \sin 2\theta$. The points on the smooth curve are the data of Authier & Warren (1956). In both experiments the brass was annealed at 500 °C. for 2 hours.

Authier & Warren (1956) measured the extinction in Fe and brass powders as a function of wavelength and concluded that their data exhibited a monotonic dependence on $\bar{Q}/\mu$ (plotted as $\lambda^3 f^2 (1+\cos^2 2\theta)\varrho/2\mu \sin 2\theta$; ϱ = density). While $\bar{Q}/\mu$ is the argument in the expression for secondary extinction in infinitely thick single crystals (equation (4)) it fails to account for the finite thickness of the single crystal grains in a powder specimen as does equation (9). We have repeated the Authier & Warren measurements and have been unable to reproduce their data nor confirm the monotonic dependence on $\bar{Q}/\mu$. Both their measurements and ours are shown in Fig. 5 for α brass. As mentioned above equation (9) offers a better description of extinction in these samples.

Summary

The mosaic block model appears to yield extinction expressions that are applicable to real crystals. Equations (4) and (8) are applicable to single crystals whose rocking curve is at least several times that of an ideally perfect crystal and equation (9) is applicable to powders. The principal value of equations (4) and (9) are their use as a guide for selecting those conditions which minimize extinction. For quantitative work equations (4) and (9) should only be employed when extinction is small.

References

Authier, A. & Warren, B. E. (1956). *J. App. Phys.* **27**, 1382.

Chandrasekhar, S. (1960). *Acta Cryst.* **13**, 588.

Darwin, C. G. (1914). *Phil. Mag.* **27**, 315, 657.

Weiss, R. J. & DeMarco, J. J. (1958). *Rev. Mod. Phys.* **30**, 59.

Zachariasen, W. H. (1944). *Theory of X-ray Diffraction in Crystals.* New York: Wiley.